



J Med Phys. 2013 Jan-Mar; 38(1): 9–14.

PMCID: PMC3607347

doi: [10.4103/0971-6203.106600](https://doi.org/10.4103/0971-6203.106600)

Dosimetric evaluation of Acuros XB dose calculation algorithm with measurements in predicting doses beyond different air gap thickness for smaller and larger field sizes

[Suresh Rana](#) and [Kevin Rogers](#)

Department of Radiation Oncology, Arizona Center for Cancer Care, Peoria, Arizona, USA

Address for correspondence: Mr. Suresh B. Rana, 14155 N. 83rd Avenue #127, Arizona Center for Cancer Care, Peoria, Arizona 85381, USA. E-mail: suresh.rana@gmail.com

Received 2012 Sep 14; Revised 2012 Dec 9; Accepted 2012 Dec 10.

Copyright : © Journal of Medical Physics

This is an open-access article distributed under the terms of the Creative Commons Attribution-Noncommercial-Share Alike 3.0 Unported, which permits unrestricted use, distribution, and reproduction in any medium, provided the original work is properly cited.

Abstract

In this study, dose prediction accuracy of Acuros XB (AXB) dose calculation algorithm beyond air gap thickness (range 2, 4, and 6 cm) in simple inhomogeneous phantoms was investigated. The evaluation of AXB was performed by comparing the doses calculated by AXB with the doses calculated by Anisotropic Analytical Algorithm (AAA) and the measured data for different field sizes (3×3 , 5×5 , and 10×10 cm²) of a 6 MV photon beam. The dose computation was performed within Eclipse treatment planning system, and measurements were acquired with a cylindrical ionization chamber. Central axis depth dose comparisons were done in solid–water material region up to 5 cm distance from air/solid–water interface. The results of AXB had better agreement with measurements at all measured points than that of AAA. The discrepancies between AXB and measured data were seen from -3.81% to $+0.9\%$, whereas the AAA differences with measurement from -3.1% to -10.9% . The combination of the smallest test field size and the largest air gap produced the highest range (1–5 cm distance from air/solid–water interface) in dose difference (AAA: -4.0% to -10.6% and AXB: -3.8% to $+0.6\%$). The AAA computational time was about 8 times faster than that of AXB. In conclusion, AXB is more appropriate to use for dose predictions, especially when low-density heterogeneities are involved.

Keywords: Anisotropic analytical algorithm, Acuros, air gap, dose prediction, heterogeneity correction

Introduction

The development of advanced cancer treatment technique such as intensity modulation radiation therapy (IMRT) has enabled the delivery of conformal dose distribution to the target while minimizing the dose to the critical structures.^[1] However, such advanced treatment technique also demands more accurate dose

calculation algorithms within the treatment planning systems (TPSs).[2] Because human body is composed of heterogeneous tissues such as bones, lungs, sinuses, and oral and nasal cavities, the characteristics of therapeutic radiation beam will be different as the beam interacts with tissues of widely differing radiological properties. Furthermore, the photon beam may pass through air gap created by the immobilization device that supports the patient on the treatment table. Hence, in order to determine the absorbed dose in the irradiated tissues more accurately, commercial TPSs must employ dose calculation algorithms that will account the presence of different media heterogeneity.[3] With regard to achieving optimum therapeutic outcome from radiation treatments, Task Group 65 (TG 65) of the American Association of Physicists in Medicine (AAPM) stated that “the general principle of 3% accuracy in dose delivery with the corresponding need for better than 2% accuracy in correcting for inhomogeneities is a reasonable, albeit challenging, goal.”[3]

The dose calculation algorithms used by clinical radiation therapy TPSs have evolved over the years from simple computations to Monte Carlo (MC) approaches. A new photon dose calculation algorithm called Acuros XB (AXB) has recently been implemented in the Eclipse TPS (Varian Medical Systems, Palo Alto, CA, USA). AXB utilizes the Linear Boltzmann Transport Equation (LBTE) and solves numerically that describes the macroscopic behavior of radiation particles as they travel through and interact with the matter. AXB is considered to be similar to MC methods for accurate modeling of dose deposition in heterogeneous media.[4]

Several validation studies on AXB have shown that the results of dose calculations from AXB were able to achieve comparable accuracy to MC methods or measurements in homogenous water medium[5] and in heterogeneous media.[4,6–9] Vassiliev *et al.*,[4] showed agreement within 2% between AXB and MC in a heterogeneous slab phantom as well as in a breast treatment plan on an anthropomorphic phantom. Bush *et al.*,[6] investigated the dosimetric accuracy of AXB with MC methods for 6 and 18 MV photon beam incident on homogenous and heterogeneous geometries, and compared the results against AAA. That study reported better agreement between MC and AXB ($\pm 3.0\%$) than between MC and AAA (up to 17.5%). Fogliata *et al.*,[7] investigated AXB in heterogeneous virtual phantoms characterized by simple geometry structures and then compared against MC and AAA. The results from that study showed that the calculated dose distributions between AXB and MC had good agreement at 6 and 15 MV photon beam. Han *et al.*,[8] reported better accuracy of AXB results when compared to the measurements in the Radiological Physics Center (RPC) head and neck phantom. Kan *et al.*,[9] showed that AAA overestimated the doses by up to 10%, while the measured doses matched those of AXB to within 3% near air/tissue interfaces in the anthropomorphic phantom.

Previous investigations[4,6,7] on the accuracy of dose predictions by AXB were mostly done by comparing AXB calculated data against MC data. In the case of comparison between AXB and measured data, the studies[8,9] were mostly focused near the tissue heterogeneity interface, and the dose prediction accuracy of AXB at multiple depths beyond different sizes of air gap remains to be addressed. The motivation of this study was to investigate the ability of AXB to calculate the dose beyond different air gap thickness by using three different field size (FS) of a 6 MV photon beam. The evaluation of AXB was done by comparing the doses calculated by AXB with the doses calculated by widely tested AAA and the measured data. In this study, the measurements were obtained in solid–water material up to 5 cm distance from the air/solid–water interface to simulate dose prediction in tumor or soft tissue that may be situated

beyond (1) small cavity inside the human body and (2) air gap created by water equivalent immobilization device. Furthermore, a comparison between the calculated and measured doses was done in the solid–water region that is located before the air gap.

Materials and Methods

AAA and AXB share the same beam model,[5,8] and configuration of AXB was done by importing the same set of beam data as used by AAA through beam configuration feature in the Eclipse TPS. The data presented in this study were taken for a 6 MV photon beam of Varian Clinac iX accelerator equipped with a Millennium 120 multileaf collimator (Varian Medical Systems, Palo Alto, CA, USA). All dose calculations and measurements were done along the central beam axis in solid–water material (1) beyond air gap up to 5 cm distance from the air/solid–water interface and (2) before air gap up to 4 cm distance from the top surface of the phantom. The test field sizes included in this study were 3×3 , 5×5 , and 10×10 cm². The source to surface distance (SSD) of 100 cm was used for depth dose computations and measurements.

Depth dose calculations Inhomogenous phantoms A (2-cm air gap), B (4-cm air gap), and C (6-cm air gap) of rectangular area 30×30 cm² were created as 3D computed tomography (CT) structure sets in the Eclipse TPS in order to simulate the experimental setup [Figure 1]. Each layer (i.e., air gap and solid–water regions) in phantoms A, B, and C had rectangular area of 30×30 cm². The phantom was defined as the body structure (CT number = 0) in order to calculate the dose. The phantoms' layers consisting of solid–water and air were assigned with CT numbers of 0 and – 1000, respectively. The central axis depth doses in all three phantoms were computed with two dose calculation algorithms implemented in the Eclipse TPS: (1) AAA, version 10.0.26 and (2) AXB, version 10.0.26.

The option to calculate either dose-to-medium (D_m) or dose-to-water (D_w) is available in AXB. For the D_m calculations in AXB, the macroscopic energy deposition cross-section and atomic density are based on the material properties of local voxel.[4–6] In contrast, the energy deposition cross-sections for water are used in place of those for the local media in the case of D_w calculations in AXB.[4–6] Han *et al.*, showed that the result of the D_m mode was found to be closer to the measurements than that of the D_w mode in AXB.[8] The option of D_m was selected for all AXB calculations in this study. For AAA, the dose is reported in D_w mode only since AAA's dose results are based on electron density scaled water.[10] The AAA accounts for the presence of heterogeneities by performing simple density scaling of MC derived kernels and secondary electron transport is only modeled macroscopically.[10–12]

For each phantom set in this study, the central axis depth doses were computed using AAA and AXB for 100 Monitor Units (MUs) using identical beam setup. The calculated (AAA and AXB) dose at each depth was then converted to the percent depth dose (PDD) by normalizing to the central axis dose at the depth of maximum dose (d_{max}). The d_{max} was obtained in the solid–water material (before the air gap) at the distance of 1.5 cm from the top surface of the phantom [Figure 1]. The dose calculation grid was set to 2.5 mm for all cases.

Depth dose measurements In order to mimic the virtual phantoms created in the Eclipse TPS, rectangular Styrofoam blocks (5×5 cm²) of thickness 2, 4, and 6 cm were placed between 5-cm thick rectangular solid–water material (30×30 cm²) above and 10-cm thick rectangular solid–water materials (30×30

cm²) below in order to create the air gaps of area $30 \times 30 \text{ cm}^2$ [Figure 1]. The Styrofoam blocks were used only as support to create the air gaps between the solid–water materials. Furthermore, the Styrofoam blocks were placed on both lateral sides of central beam axis such that no radiation field used in this study would irradiate the Styrofoam.

By keeping identical field, beam parameters and geometries that were used for dose computation by AAA and AXB in the Eclipse TPS, 100 MUs were delivered to the phantoms, and central axis depth dose measurements were acquired with Exradin A1 cylindrical ionization chamber (Standard Imaging, Middletown, WI). The measurement at each depth was repeated three times and an average of three electrometer readings (nC) was converted to the measured PDD by normalizing to the central axis dose obtained at the distance of 1.5 cm from the top surface of the phantom; this allowed having the same dose normalization point for depth dose computations and measurements.

Computational time The computational time was recorded for AAA and AXB calculations in the Eclipse TPS that was installed on a CITRIX workstation (Dell PowerEdge R610) with Intel (R) Xeon (R) 2.67-GHz processor, 48-GB RAM memory, and a 32-bit Microsoft® Windows Server® Standard operating system.

Results

Percent depth dose comparison Figure 2 shows the measured PDDs at selected points of interest as well as the calculated PDD curves by AAA and AXB in phantoms A (2-cm air gap thickness), B (4-cm air gap thickness), and C (6-cm air gap thickness) for field sizes 3×3 , 5×5 , and $10 \times 10 \text{ cm}^2$. Figure 3 shows the dose difference (Δ) in percentage between the calculated (AAA and AXB) and measured PDD data in phantoms A, B, and C for field sizes 3×3 , 5×5 , and $10 \times 10 \text{ cm}^2$. In Figure 3, the Y-axis represents the dose difference in percentage, whereas X-axis represents the distance (cm) of measured point from the air/solid–water interface. The Δ (%) was calculated using equation (1).

$$\Delta (\%) = \left(\frac{\text{Calculated (AXB or AAA) PDD} - \text{Measured PDD}}{\text{Measured PDD}} \right) \times 100 \quad (1)$$

The negative dose difference ($-\Delta$) and the positive dose difference ($+\Delta$) mean, the dose underprediction and overprediction, respectively, by the dose calculation algorithm (AAA or AXB).

The results from Figure 2 show that both AXB and AAA predicted doses within $\pm 1\%$ of the measured doses in the first solid–water region (i.e., upstream of air gap). However, it can be seen from Figure 3 that AXB's values had better agreement (smaller absolute value of Δ) with the measurements at all measured points beyond air gaps than that of AAA, and this was true for all three test field sizes. Specifically, AXB predicted doses within $\pm 1\%$ of measured doses except at 1 cm distance from the air/solid–water interface in phantom B ($\Delta = -2.9\%$; FS = $3 \times 3 \text{ cm}^2$) and in phantom C ($\Delta = -3.8\%$; FS = $3 \times 3 \text{ cm}^2$ and $\Delta = -1.5\%$; FS = $5 \times 5 \text{ cm}^2$). The AAA underpredicted the doses at all measured depths in three phantoms regardless of the field size used. The combination of smallest test field size (i.e., $3 \times 3 \text{ cm}^2$) and the largest air gap (i.e., 6-cm thickness) produced the highest range (between 1 and 5 cm from air/solid–water interface) in dose difference (AAA: -4.0% to -10.6% and AXB: -3.8% to $+0.6\%$). Furthermore, the discrepancies

between AAA and measured data was minimum at 1 cm from the air/solid–water interface and their dose discrepancies ($-\Delta$) continued to increase as the distance of measurement point from the air/solid–water interface increased. A similar trend could not be identified between the results of AXB and measurements.

Computational time comparison Table 1 shows the computational time for the AAA and AXB calculations. The AAA computation time was faster than that of AXB. Specifically, in comparison to AXB computation time, the AAA computation time was 5-6 times faster for a field size $3 \times 3 \text{ cm}^2$, 5-8 times faster for a field size $5 \times 5 \text{ cm}^2$, and 10-17 times faster for a field size $10 \times 10 \text{ cm}^2$.

Discussion

In this study, the dose calculation accuracy of AXB has been evaluated with respect to measurement. Our results indicated that AXB was superior to AAA in predicting doses beyond air gaps as compared against measured data. Similar observation was reported in previous investigations showing that AXB was more accurate to use for dose computations in heterogeneous media than AAA by comparison against measurements or MC calculations.[4,6–9] Although AXB had good agreement with the measurements, higher dose discrepancies were still observed nearby the air/solid–water interface in the phantom with a larger air gap thickness. Increasing the air gap between two solid–water materials will cause reduction in scattered radiation reaching the measurement point downstream due to lateral spread of scattered radiation within the air gap.[3] Such higher dose discrepancies (up to -3.8%) in AXB may be due to its inability to estimate the scattered radiation contribution to the measurement points in the second build-up and build-down regions beyond low-density medium like air, especially for a small field size.

Several researchers found that the secondary build-up region occurred beyond air cavities in the interface region to re-establish electronic equilibrium.[6,7,11,12,13,14] Bush *et al.*, showed that AXB differences with MC results up to 4.5% in the secondary build-up beyond the air for 6 MV photon beam of field size $10 \times 10 \text{ cm}^2$. [6] Thus, although the results of this study suggest that AXB is more accurate than AAA, the dose differences more than $\pm 2\%$ could still result when using AXB to calculate the dose for a 6 MV photon beam of small field size that passes through large air gap or cavity.

The dose difference as a function of field size was evaluated in all three phantoms. At 1 cm distance from the air/solid–water interface in phantom C (6-cm air gap thickness), the dose difference between AXB, and measurement was improved from -3.8% to -1.5% to -0.2% when field size was increased from $3 \times 3 \text{ cm}^2$ to $5 \times 5 \text{ cm}^2$ to $10 \times 10 \text{ cm}^2$, respectively. However, by changing the field size, no discernible trend could be identified in the results between AXB and measurements at other measurement points regardless of the choice of phantom.

In contrast, at a given measurement point between 2 and 5 cm distance from the air/solid–water interface, dose differences between AAA and measurements were improved by average values of 2.7% (2.5-3.1%) in phantom A, 3.8% (3.7-4.1%) in phantom B, and 4.3% (4.0-4.6%) in phantom C when the field size was increased from $3 \times 3 \text{ cm}^2$ to $10 \times 10 \text{ cm}^2$. A similar trend could not be identified in the results of AAA and measurement at 1 cm from the air/solid–water interface in a given phantom. These results indicated that the dose prediction by AAA and AXB is dependent on the combination of field size, thickness of air gap, and location of measurement point from the air/solid–water interface.

Kan *et al.*, reported that AAA could only predict little secondary build-up beyond the air.[9] Bush *et al.*,

showed that dose difference between AAA and MC results was up to 13% in the secondary build-up beyond the air using a $10 \times 10 \text{ cm}^2$ 6 MV photon beam.[6] However, in our study, dose prediction against measurements was evaluated between 1 and 5 cm from the air/solid–water interface, and AAA underpredicted the dose by up to -10.9% in the solid–water material beyond air gap. The dose underprediction by AAA may be due to approximations employed within AAA that takes heterogeneity into account by applying density-based correction to dose kernels calculated in water.[9,10] Furthermore, media of different density causes electron disequilibrium at and near their heterogeneity interface, and the effect due to electron disequilibrium in AAA is approximated by an empirical convolution along a ray line.[9,10] Such approximations in AAA may result in the underestimation of build-up and build-down effects near the interfaces in the presence of air.[9,10]

Although dose measurements within the air gap were not conducted in this study, it is evident from [Figure 2](#) that clear dose discrepancies exist between the results of AXB and AAA in the air gap as well as at the air/solid–water interface. Comparison between the measured and calculated doses (AXB and AAA) in the air gap region of various thicknesses will be an interesting topic for future studies. In summary, the results of our study showed that AXB is more appropriate for dose calculation if the photon beam traverses the air gap created by water equivalent immobilization device prior to entering the patient. Furthermore, AXB is also more appropriate in dose predictions especially when tumor is situated next to low-density tissues such as lung and esophagus inside the human body. Further verification of dose prediction accuracy of AXB must be performed in different clinical situations. For instance, the discrepancies between calculated (AXB) and measured doses may also occur when the photon beam passes through a high-density immobilization device prior to entering the patient and then finally reaching the deep-seated tumor next to the bone. Future work involves clinically relevant measurements in complex phantoms to investigate how multiple tissue heterogeneities (combination of low- and high-density media) would affect the dose predictions by AXB. The dosimetric impact on real CT data of different treatment sites due to dose recalculation from AAA to AXB must be investigated too.

Conclusion

The dose prediction accuracy of AXB beyond different sizes of air gap in simple geometric circumstances was assessed by comparing calculated data of AXB against experimental measured data for a 6 MV photon beam. The results of this study showed that AXB was superior to AAA in dose predictions beyond air gaps/cavities when compared against the measurements. Based on the results reported in this study, AXB is more appropriate to use for dose calculation especially when low-density heterogeneities are involved. An effort must be made to avoid large air gaps created by immobilization devices when smaller field sizes are used for the radiation treatment.

Footnotes

Source of Support: Nil

Conflict of Interest: None declared

References

1. Otto K. Volumetric modulated arc therapy: IMRT in a single gantry arc. *Med Phys*. 2008;35:310–7.

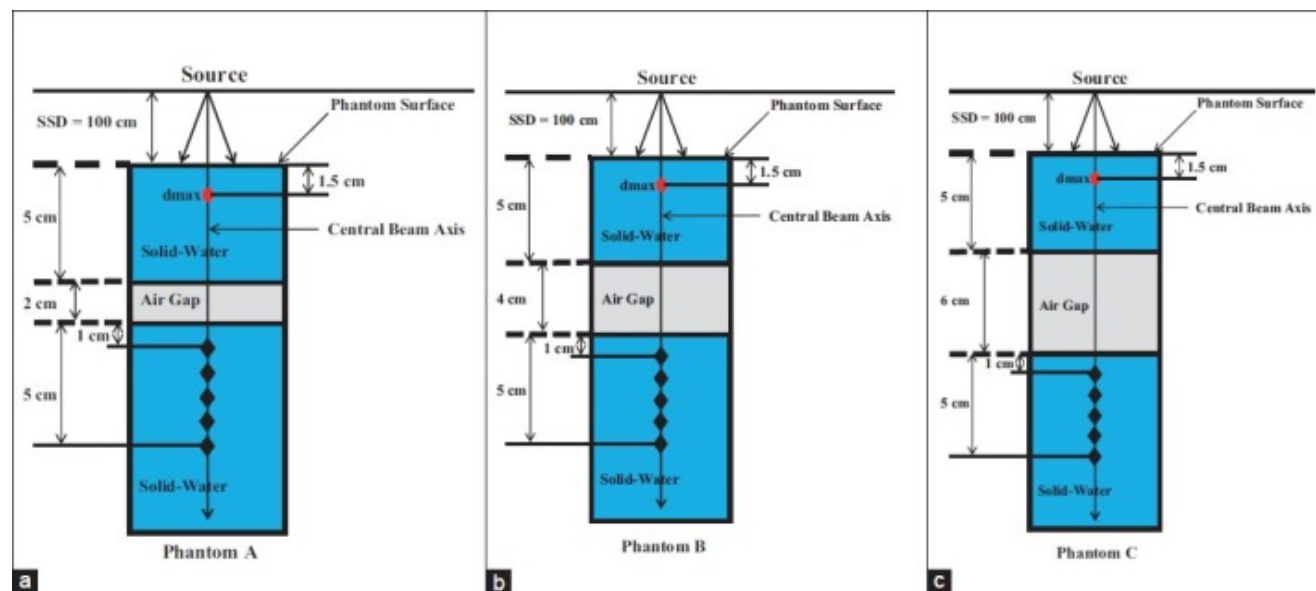
[PubMed: 18293586]

2. Das IJ, Ding GX, Ahnesjö A. Small fields: Nonequilibrium radiation dosimetry. *Med Phys*. 2008;35:206–15. [PubMed: 18293576]
3. Papanikolaou N, Battista JJ, Boyer AL, Kappas C, Klein C, Mackie TR, et al. Tissue inhomogeneity corrections for megavoltage photon beams. Report of Task Group No. 65 of the Radiation Therapy Committee of the American Association of Physicist in Medicine. AAPM Report No. 85. [Last accessed on Aug 15, 2012]. Available from: http://www.aapm.org/pubs/reports/rpt_85.pdf.
4. Vassiliev ON, Wareing TA, McGhee J, Failla G, Salehpour MR, Mourtada F. Validation of a new grid based Blotzmann equation solver for dose calculation in radiotherapy with photon beams. *Phys Med Biol*. 2010;55:581–98. [PubMed: 20057008]
5. Fogliata A, Nicolini G, Clivio A, Vanetti E, Mancosu P, Cozzi L. Dosimetric validation of Acuros XB Advanced Dose Calculation algorithm: Fundamental characterization in water. *Phys Med Biol*. 2011;56:1879–904. [PubMed: 21364257]
6. Bush K, Gagne IM, Zavgorodni S, Ansbacher W, Beckham W. Dosimetric validation of Acuros XB with Monte Carlo methods for photon dose calculations. *Med Phys*. 2011;38:2208–21. [PubMed: 21626955]
7. Fogliata A, Nicolini G, Clivio A, Vanetti E, Cozzi L. Dosimetric evaluation of Acuros XB Advanced Dose Calculation algorithm in heterogeneous media. *Radiat Oncol*. 2011;6:82. [PMCID: PMC3168411] [PubMed: 21771317]
8. Han T, Mourtada F, Kisling K, Mikell J, Followill D, Howell R. Experimental validation of deterministic Acuros XB algorithm for IMRT and VMAT dose calculations with the Radiological Physics Center's head and neck phantom. *Med Phys*. 2012;39:2193–202. [PMCID: PMC3337663] [PubMed: 22482641]
9. Kan MW, Leung LH, Yu PK. Verification and dosimetric impact of Acuros XB algorithm on intensity modulated stereotactic radiotherapy for locally persistent nasopharyngeal carcinoma. *Med Phys*. 2012;39:4705–14. [PubMed: 22894395]
10. Sievinen J, Ulmer W, Kaissl W. AAA photon dose calculation in Eclipse. Varian documentation RAD #7170B. 2005
11. Van Esch A, Tillikainen L, Pyykkonen J, Tenhunen M, Helminen H, Siljamäki S, et al. Testing of the analytical anisotropic algorithm for photon dose calculation. *Med Phys*. 2006;33:4130–48. [PubMed: 17153392]
12. Robinson D. Inhomogeneity correction and the analytic anisotropic algorithm. *J Appl Clin Med Phys*. 2008;9:2786. [PubMed: 18714283]
13. Wong TP, Kan WK, Law M. The effects of air cavities on X-ray dose distribution at 6 and 25 MV. *Australas Phys Eng Sci Med*. 1996;19:237–47. [PubMed: 9060210]
14. Shahine H, Al-Ghazi MS, El-Khatib E. Experimental evaluation of interface doses in the presence of

air cavities compared with treatment planning algorithms. Med Phys. 1999;26:350–5.

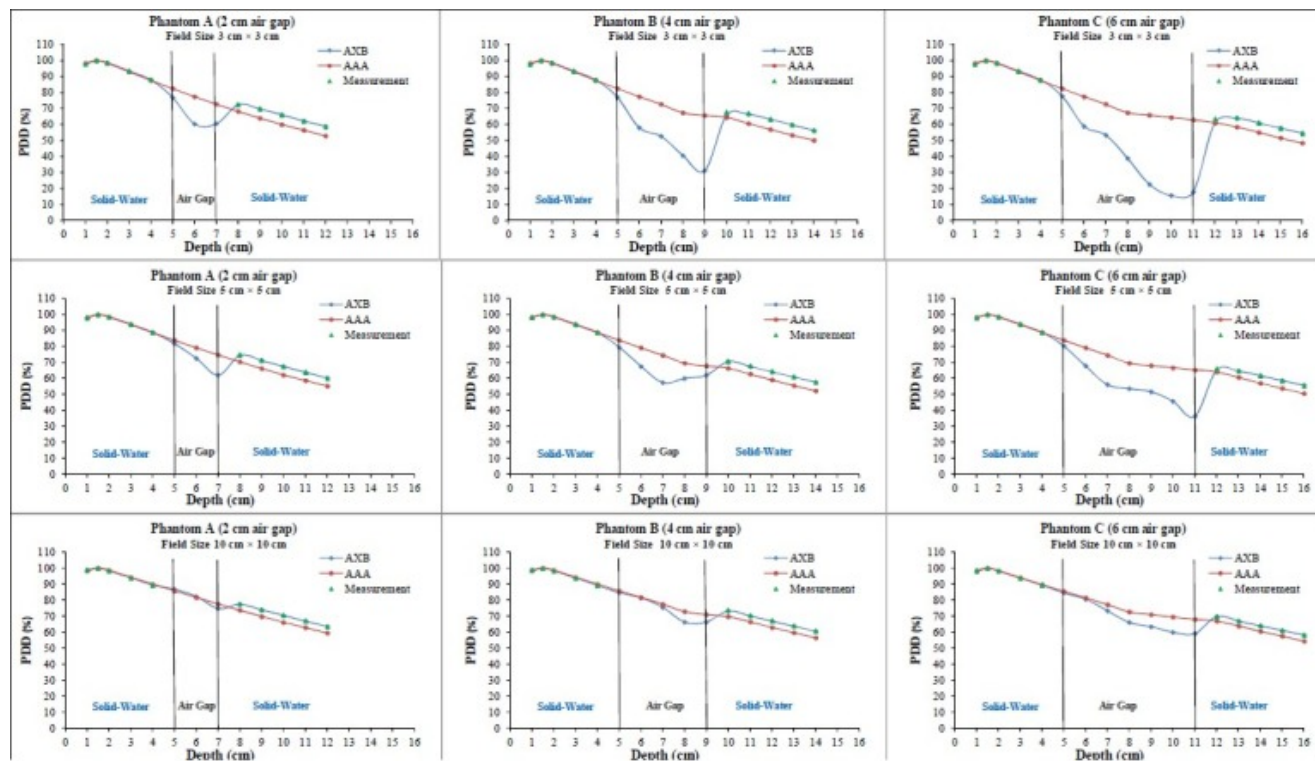
Figures and Tables

Figure 1



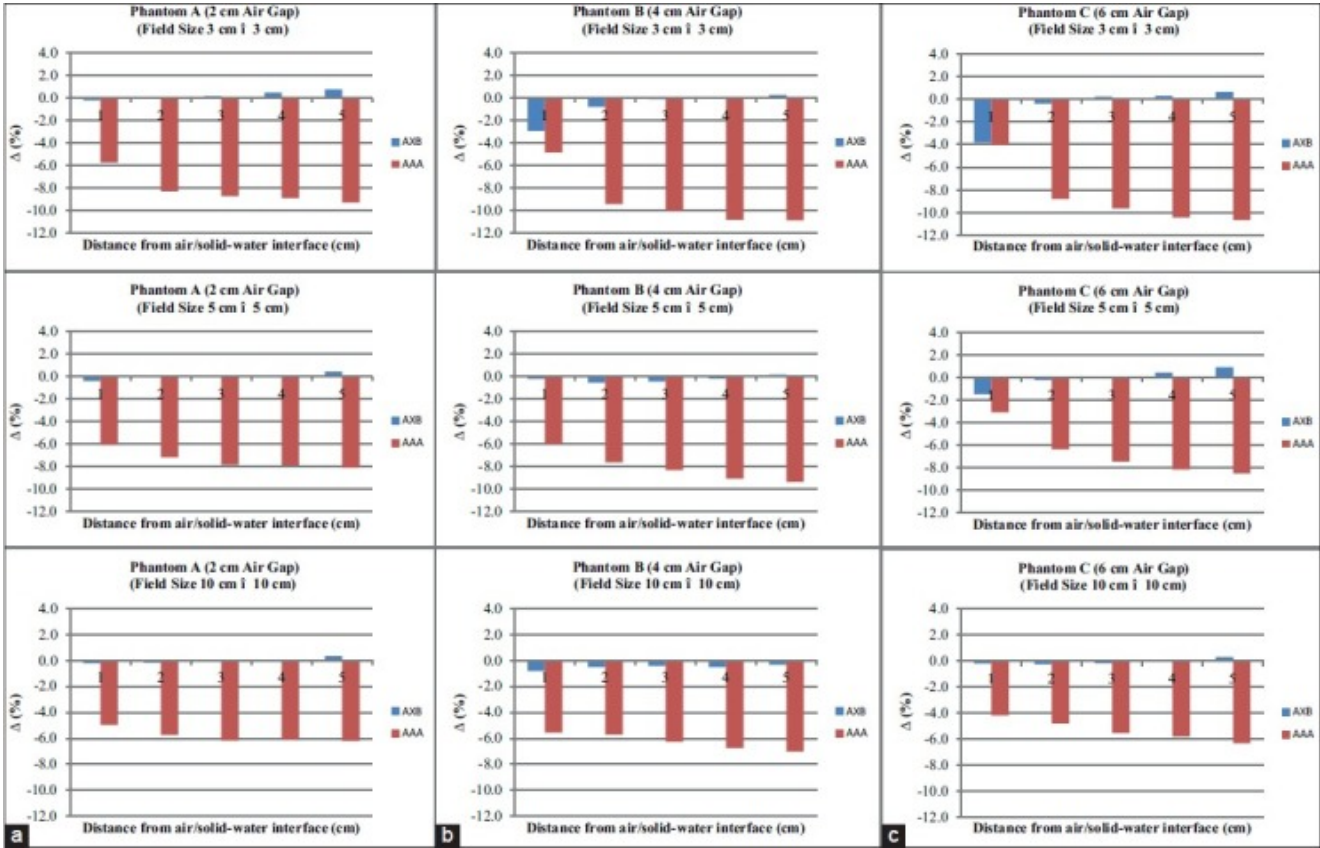
(a) schematic of the experimental setup for depth dose computations and measurements in phantom A (2-cm air gap), phantom, (b) (4-cm air gap), and phantom, (c) (6-cm air gap) (from left to right). Each layer (i.e., air gap and solid–water regions) in phantoms A, B, and C had rectangular area of $30 \times 30 \text{ cm}^2$. Central axis depth doses were compared in the first solid–water region (upstream of air gap) and second solid–water region (downstream of air gap). The common normalization point [i.e., depth of maximum dose (d_{max}) = 1.5 cm] that was used for dose computations and measurements is marked with red dot

Figure 2



The measured PDD in the solid-water regions (upstream and downstream of air gap) and the calculated PDD curves by AAA and AXB in phantoms A (2-cm air gap), B (4-cm air gap), and C (6-cm air gap), (from left to right) for field sizes 3×3 , 5×5 , and $10 \times 10 \text{ cm}^2$ (from top to bottom). (6 MV photon beam, 100 cm SSD, 100 MUs). Abbreviations: PDD = Percent Depth Dose, AAA = Anisotropic Analytical Algorithm, AXB = Acuros XB Algorithm, SSD = Source to Surface Distance, MUs = Monitor Units.

Figure 3



Comparisons between calculated and measured PDD at points between 1 and 5 cm distance from the air/solid–water interface in phantoms A (2-cm air gap), B (4-cm air gap), and C (6-cm air gap), (from left to right) for field sizes 3 × 3, 5 × 5, and 10 × 10 cm² (from top to bottom). The Δ (%) was calculated using Equation 1. (6 MV photon beam, 100 cm SSD, 100 MUs).Abbreviations: AAA = Anisotropic Analytical Algorithm, AXB = Acuros XB Algorithm, PDD = Percent Depth Dose, Δ (%) = Dose Difference, SSD = Source to Surface Distance, MUs = Monitor Units.

Table 1

	<i>Field size (cm²)</i>	<i>Computational time (S)</i>	
		<i>AAA</i>	<i>AXB</i>
Phantom A (2-cm air gap)	3×3	7	41
	5×5	7	53
	10×10	9	149
Phantom B (4-cm air gap)	3×3	9	46
	5×5	10	57
	10×10	12	142
Phantom C (6-cm air gap)	3×3	9	48
	5×5	11	60
	10×10	14	146

AAA=Anisotropic analytical algorithm, AXB=Acuros XB algorithm

Computational time (in seconds) of anisotropic analytical algorithm and acuros XB algorithm for dose calculations in phantoms A, B, and C

Articles from Journal of Medical Physics are provided here courtesy of **Wolters Kluwer -- Medknow Publications**